

A toy model to understand the dynamics of the vortical motions in turbulent boundary layers

J.C. Cuevas Bautista*

University of New Hampshire, Department of Mechanical Engineering, Durham 03824, USA.

(Dated: April 26, 2016)

Recent studies indicate that the structure of the turbulent boundary layer at high Reynolds number (Re) is composed of large uniform momentum zones segregated by fissures of concentrated vorticity. Experiments reveal that the dimensionless fissures thickness (scaled by boundary layer thickness) is $\mathcal{O}(1/\sqrt{Re})$ and the dimensionless streamwise velocity jump across a fissure scales with the friction velocity $\mathcal{O}(u_\tau)$. A toy model that captures the essential elements of the turbulent boundary layer structure at high Re is constructed to evaluate the long-time averaged flow statistics of the boundary layer. First, a “master” instantaneous streamwise velocity profile in the wall-normal direction is constructed by placing a discrete number of fissures across the boundary layer thickness. The number of fissures and their wall-normal locations follow scalings informed by the Mean Momentum Balance (MMB) theory. Next, the wall-normal positions of the fissures are allowed to randomly move in the wall-normal direction creating a statistically independent second instantaneous velocity profile. This process is then repeated to create an ensemble of instantaneous velocity profiles from which average statistics of the turbulent boundary layer can be computed and assessed. The statistics of the toy model are compared to statistics acquired in turbulent boundary layers at high Re .

I. INTRODUCTION

Turbulent boundary layer and its mechanism is one the most active research area in fluid mechanics. Due to its chaotic behaviour, deterministic approaches are not possible. However there is a general consensus in the scientific community about that turbulent boundary layers exhibit similar statistical properties. One of the stronger hypothesis support the idea that the smoothness in the average of the streamwise velocity profile is caused by the spatial average of multiple instantaneous velocity profiles with different zones of uniform momentum [1, 2]. In this article a toy model is attempted to demonstrate this assertion. The mean streamwise velocity profile is reproduced by average different instantaneous velocity profiles with a different distribution of uniform momentum zones. The phenomenological description of the structure of the uniform momentum zones through the boundary layer has been studied by several authors [?]. They suggest that UMZ are the result of the interaction of the wider range of structures that populate the turbulent boundary layer[?] such as hairpins and streamwise vortices. [3] Adrian, Meinhart and Tomkins have made a thoroughly study about how these structures segregate the UMZs. These studies indicate that theses regions of uniform momentum are segregated by smaller structures named vortical fissures.[4] Priyadarshana does a good description of what a vortical fissure looks like and how they can be distributed in the mean velocity profile. These studies revels that vortical fissures are also a representation of a more complex 3d structures called eddies. Though a numerical model to explain these interactions is further away to be developed since these occurs at high

Reynolds numbers and DNS simulations are still limited to lower Reynolds Numbers, experimental data is available but it can be overwhelming analyse such amount of information and also it is use to be very rigid to explore different parameters due a lacking of a theoretical model. Adrian, marusic, etc talks about the eddies are created and move trough the boundary layer. A vortical fissure can be seen like the signature of a hairpin vortex in the streamwise-wall-normal plane(figure). [3] Adrian and other has studied throughly how this vortex structures organize in turbulent flows.

II. NUMERICAL METHODS

A step master stream-wise velocity profile is represented by a set of discrete steps uniformly spaced according with Eqs. 1 and 2,

$$U_{i+1}^+ = U_i^+ + \phi_c^2 \ln(\phi_c), \quad (1)$$

$$y_{i+1}^+ = \phi_c y_i^+. \quad (2)$$

These relationships are derived from the MMB theory [5], where Eq. 1 determine the increments in the stream-wise normalized velocity U^+ , the width of the steps in the x coordinate and Eq. 2 determine the increments in the normalized wall normal position y^+ , the height of the steps in the y coordinate (See Fig. 1). The constant factor ϕ_c is given by $\phi_c = (1 + \sqrt{5})/2$ and since the thickness of the vortical fissures scales like $\mathcal{O}(1/\sqrt{Re})$, it is considered negligible at high Re . The initial wall normal position was set to $y_0^+ = \phi_c \sqrt{\delta^+}$ in order to match with the onset of the logarithmic region according with the MMB theory and $U_0^+ = 0.5 U_\infty^+$ to be the half of the normalized free-stream velocity U_∞^+ .

* jcc1@wildcats.unh.edu

The last position y_N^+ of the vortical fissure and its associated velocity U_N^+ is bounded by the turbulent boundary layer thickness δ or its respective Reynolds number $\delta^+ = \frac{\delta}{\nu/u_\tau}$, where $u_\tau = \sqrt{\tau_\omega/\rho}$ is the friction velocity (τ_ω is the mean wall shear stress and ρ is the mass density respectively) and ν is the kinematic viscosity. Fig. 1 depicts the step master turbulent velocity profile with a grid of 5481 linearly spaced positions in the wall normal direction each one associated to a streamwise velocity. The dot circles are the positions and velocities of the vortical fissures computed using Eqs. 2 and 1 respectively. The zones of uniform momentum are created allocating the same velocity of the vortical fissure to the grid points between the previous vortical fissure and the current vortical fissure. This velocity remains characteristic for each vortical fissure, thus the number of vortical fissures establishes the number of uniform momentum zones.

Then instantaneous multiple velocity profiles are created by simulate a random motion in the wall normal direction of the vortical structures. This is accomplished by add a Gaussian perturbation of the actual height of the uniform momentum zone to the current position of the vortical fissure (black dots in Fig. 1) in the step turbulent master profile. Once the new wall normal positions have been computed, the grid velocity is filled with the attached velocity of each vortical fissure corresponding to their new wall normal positions. This physically means that the vortical fissures can cross each other through the turbulent boundary layer step profile generating zones of negative vorticity. Fig. 2 shows five instantaneous turbulent velocity step profiles, it can be seen how the vortical fissures changes their position trough the turbulent boundary layer for the different profiles. The time units in Fig. 2 are arbitrary, i.e. they just illustrate different instants of time. The multiple instantaneous step velocity profiles are considered independent events since they are the result of the Gaussian perturbation in the wall

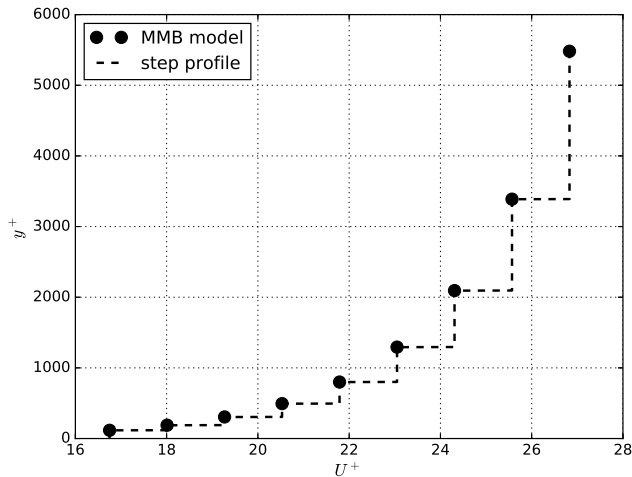


FIG. 1. Step turbulence master profile for $\delta^+ = 5200$ and $U_\infty^+ = 26.5$.

normal positions of the master profile. Thus to achieve statistical convergence the mean turbulent stream-wise velocity profile is constructed by average over 5000 independent realizations.

III. MEAN TURBULENCE STATISTICS ANALYSIS

For the purpose of validate the toy model, the high order moments such as the mean, variance, skewness and kurtosis of the mean turbulent streamwise velocity profile were computed. As described in Sec. II, not only a Gaussian perturbation was used to randomize the positions of the vortical fissure but also an uniform distribution. These variations attempts to explore if there is a dependence between the perturbation distribution and the statistics of the toy model. Thus a strong agreement between the numerical results either for any perturbation and the experimental data could give us some insight about the statistical nature of this process in a real turbulent flow.

A. Gaussian perturbation

Multiple scenarios with different standard deviations were investigated for the Gaussian perturbation, however just two are presented here. They represent poor $\sigma = 0.4$ and good $\sigma = 1$ agreement with the experimental results [6, 7], both with $\mu = 0$. First scenario considers that the random variation in the position of the vortical fissures ranges between -120% and 120% of their current positions, where 3σ events are less likely to occur. Fig. 3 is the turbulent mean velocity profile for $\sigma = 0.4$. It can be appreciated regions of relative uniform

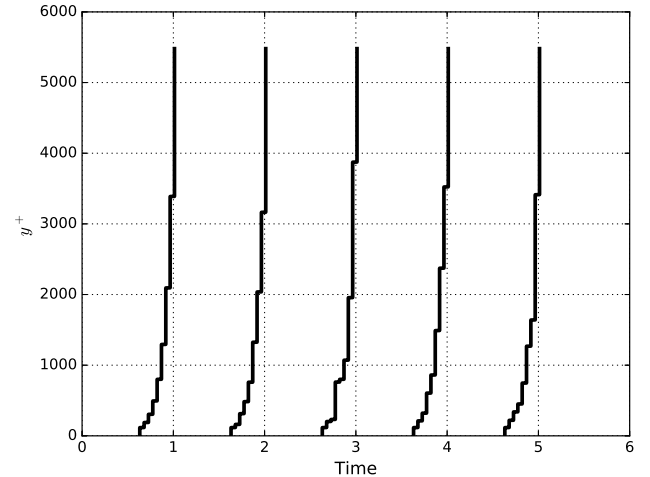


FIG. 2. Multiple instantaneous velocity profiles with a gaussian perturbation of mean $\mu = 0$ and standard deviation $\sigma = 0.4$.

velocity along with small velocity jumps located close to the unperturbed wall normal positions of the vortical fissures (see Fig. 1). These oscillations are similar to the peak-locking phenomena in experimental data, and they are the result of the velocity average of vortical fissures with identical velocities in the same wall normal positions. Also note that an uniform momentum zone arise from $y^+ = 0$ to $y^+ = 118$, these are the velocity boundary conditions imposed in the first position of the vortical fissure which are held fixed. Despite of these discrepancies, the mean velocity profile shows an acceptable agreement with the shape of the experimental data.

Fig. 4 shows the variance of the streamwise fluctuations for 5000 independent realizations as a function of the wall normal position. Here the peak-locking phenomena is more evident and it could be associated to the use of pseudo-random number generators (PRNG). Since the Gaussian random numbers are not totally independent but they are computed through a deterministic algorithm, wall normal positions can be populated with the same vortical fissures several times [8]. It is also remarkable that for this scenario crossing vortical fissures are rarely observed since the random perturbation does not exceed 130% units of their current wall normal positions.

As is usual Fig. 5 shows the skewness for the streamwise fluctuations as a function of the wall normal position on a semi-logarithmic axes plot. The graph shows the correct trend in the lower and the upper edge of the inertial region (Layer III table), i.e. it is maximum in the proximity of the wall and then it reaches its maximum negative value close to the boundary layer thickness $y^+ = \delta^+$. However through the inertial region the skewness oscillates with an small amplitude ± 1 around the value for a Gaussian distribution, in contrast with the experimental data that shows a plateau tendency

right below of the Gaussian trend. The abrupt variations in the skewness can be also a side effect of peak-locking. Unlike the skewness, the oscillations for the stream-wise velocity kurtosis (Fig. 6) have a higher amplitude trough the inertial region where the experimental data exhibit an uniform subgaussian trend. This behaviour does not reproduce properly the turbulence statistics and thus we explore higher values of σ in the Gaussian perturbation.

In the second scenario $\sigma = 1$ is selected in order to achieve a more homogeneous velocity distribution. This perturbation creates a random vertical motion of the vortical fissures between -300% and 300% of their respective step height (see Sec. II). Consequently the vortical fissures in the upper edge of the inertial region can cross and reside close to the wall. The opposite is also true for vortical motions that lie in the onset of the inertial region. Fig. 7 shows a smoother profile compared with $\sigma = 0.4$ where peak-locking effect was still present. This mean velocity profile exhibits a good agreement for $\delta^+ = 5200$ respect to the experimental data. In addition to the mean, the second, third and fourth order moments are also computed for this scenario. Fig. 8 reveals some of the main properties of the stream-wise velocity variance for turbulent flows. These are the variance is zero in the vicinity of the wall with its maximum value in the onset of the logarithmic region and then decreases almost logarithmically toward the boundary layer edge $y^+ = \delta^+$. Although the variance is not totally smooth, it is a good improvement over the variance for the first scenario. Also note there is not evidence of peak-locking effect like can be visualized in the third and fourth moments (Figs. 9 and 10). Fig. 9 shows the skewness for $\sigma = 1$, it can be appreciated how the skewness has its maximum positive value close to the wall and then when it is approaching to the log region exhibits a subgaus-

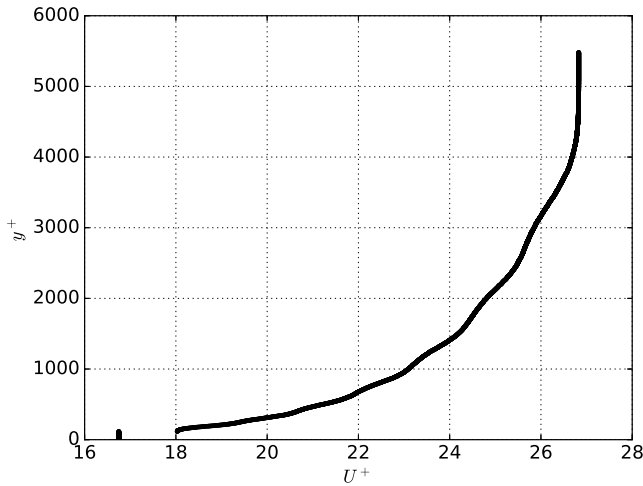


FIG. 3. Mean stream-wise velocity profile for 5000 independent realizations with a Gaussian perturbation of $\mu = 0$ and $\sigma = 0.4$.

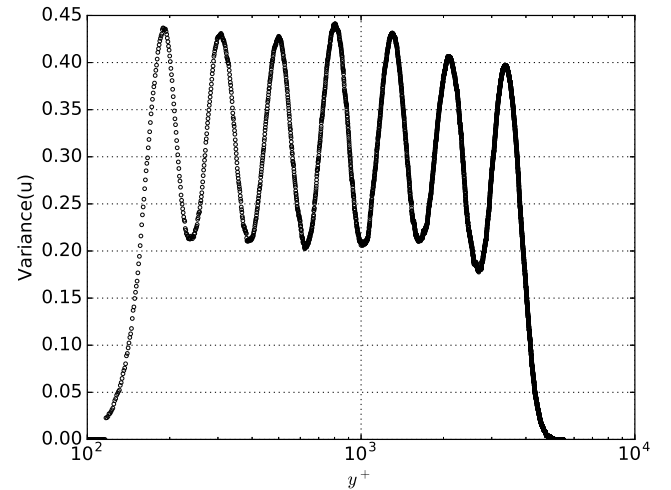


FIG. 4. Stream-wise velocity variance for 5000 independent realizations with a Gaussian perturbation of $\mu = 0$ and $\sigma = 0.4$.

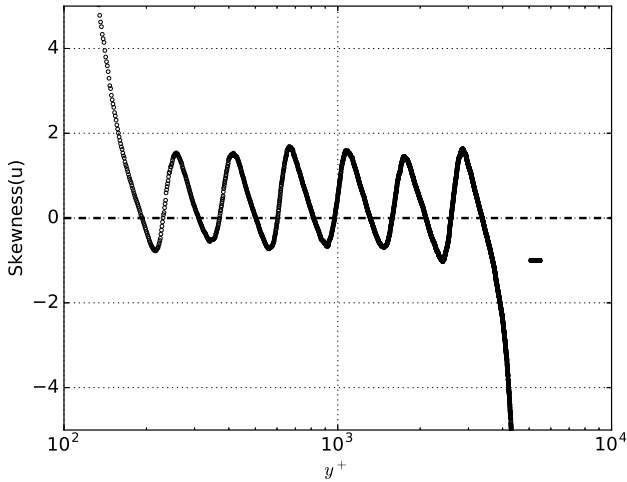


FIG. 5. Skewness of streamwise velocity fluctuations for 5000 independent realizations with a Gaussian perturbation of $\mu = 0$ and $\sigma = 0.4$ (open circles). The skewness for a Gaussian distribution is plotted in dotted lines as reference.

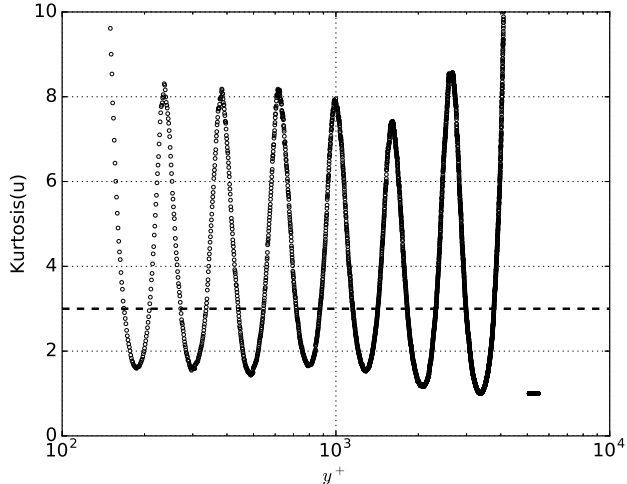


FIG. 6. Kurtosis of streamwise velocity fluctuations for 5000 independent realizations with a Gaussian perturbation of $\mu = 0$ and $\sigma = 0.4$ (open circles). The kurtosis for a Gaussian distribution is plotted in dotted lines as reference.

sian trend that rapidly decays to its maximum negative peak at the end of the logarithmic region. Unlike the experimental results, the boundaries of the skewness in the toy model still do not show the adequate trend. This is caused mainly because the first and last step vortical positions in the model are not being perturbed. Further investigation is necessary to establish the proper boundary conditions in order to improve the agreement near to the wall and away from it in the boundary layer for the turbulent statistics. Observation of Fig. 10 evidences a similar pattern for the streamwise kurtosis, where the behaviour of the trend in the boundaries does not reproduce the experimental results faithfully. Despite of

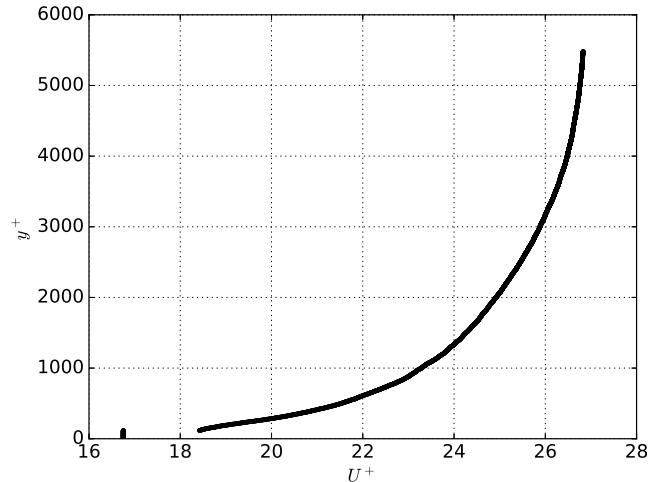


FIG. 7. Mean turbulent stream-wise velocity profile for 5000 independent realizations with a Gaussian perturbation of $\mu = 0$ and $\sigma = 1$.

these discrepancies the kurtosis is very well behaved in the inertial region where it exhibits a subgaussian trend just as the real data do. Experimentally it is expected that the kurtosis reach its maximum value at $y^+ = \delta^+$ and then decay in the free-stream region outside to the boundary layer. This is not observed in our results due to the boundary conditions explained previously. However a new distribution to perturb the position of the vortical fissures is attempted, one whose edges decays smoother than the gaussian distribution, thus a dependence on the perturbation distribution can be discarded. Next section describe the numerical results of the turbulence statistics using an uniform distribution.

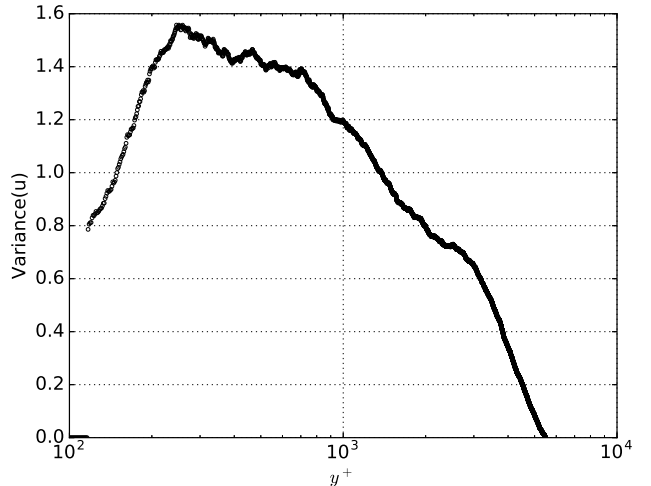


FIG. 8. Stream-wise velocity variance for 5000 independent realizations with a Gaussian perturbation of $\mu = 0$ and $\sigma = 1$.

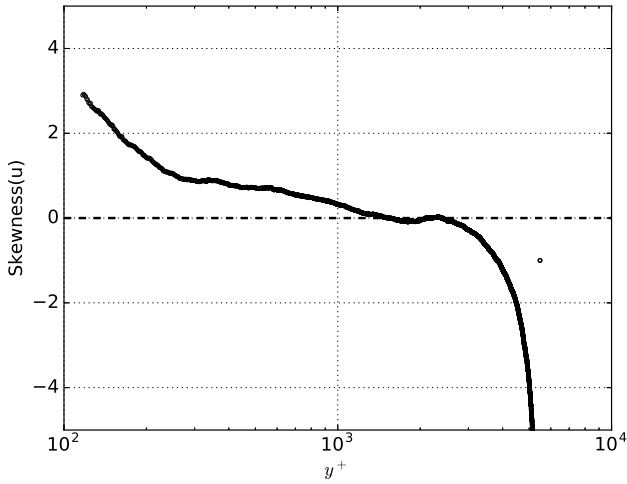


FIG. 9. Skewness of streamwise velocity fluctuations for 5000 independent realizations with a Gaussian perturbation of $\mu = 0$ and $\sigma = 1$ (open circles). The skewness for a Gaussian distribution is plotted in dotted lines as reference.

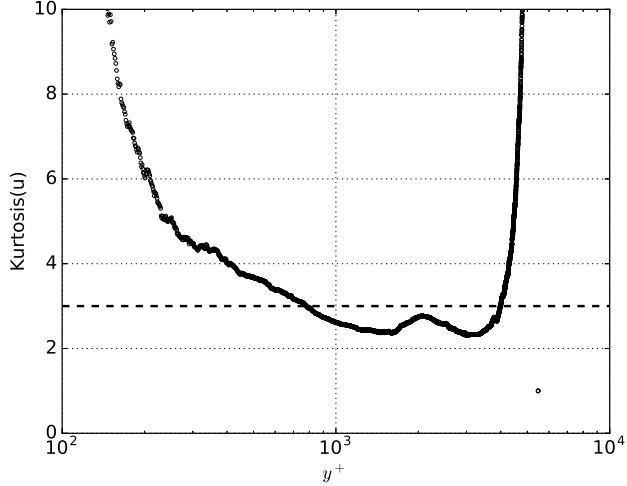


FIG. 10. Kurtosis of streamwise velocity fluctuations for 5000 independent realizations with a Gaussian perturbation of $\mu = 0$ and $\sigma = 1$ (open circles). The kurtosis for a Gaussian distribution is plotted in dotted lines as a reference.

B. Uniform distribution

Previous section suggest that the vortical fissure crossing enhances the creation of a more homogeneous velocity distribution in the boundary layer, therefore an uniform distribution between -130% and 130% of the height of the step has been selected. Fig. 11 shows the streamwise velocity profile for the uniform perturbation. In comparison with Fig 3, the jumps in the velocity profile seems to have a more straight slope. Since for an uniform distribution, all the vortical positions have the same probability to occur, regions of concentrated velocity such like in the gaussian distribution are not observed. Instead zones

with an increasing uniform velocity are appreciated. This

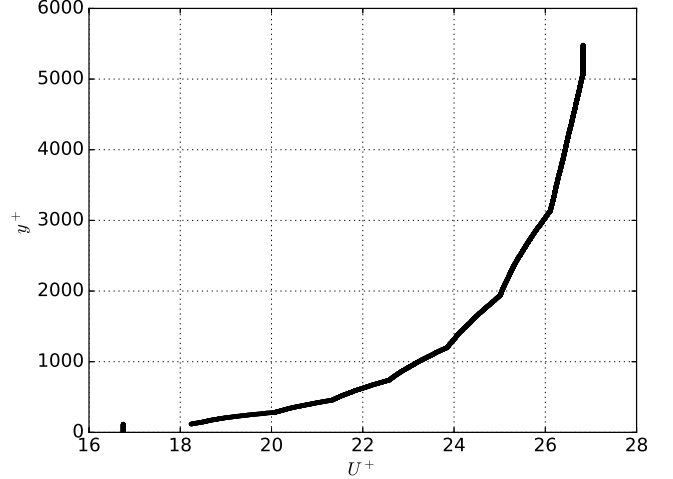


FIG. 11. Mean turbulent stream-wise velocity profile for 5000 independent realizations with an uniform perturbation of $\pm 130\%$.

effect can be appreciated more clearly in the stream-wise velocity variance (Fig. 12), where the variance oscillates around the positions of the vortical fissures in the master profile. These oscillations are characterized by having a smaller amplitude (~ 0.2 units) compared with the Gaussian perturbation for $\sigma = 0.4$ (Fig. 4). Despite of the oscillations, the main features of the turbulence variance are conserved. For instance it has a peak in the proximity of the wall and then a pronounced negative slope in the inertial region up to reach zero in the upper edge of the inertial region.

The rapid variations still persist in the higher order

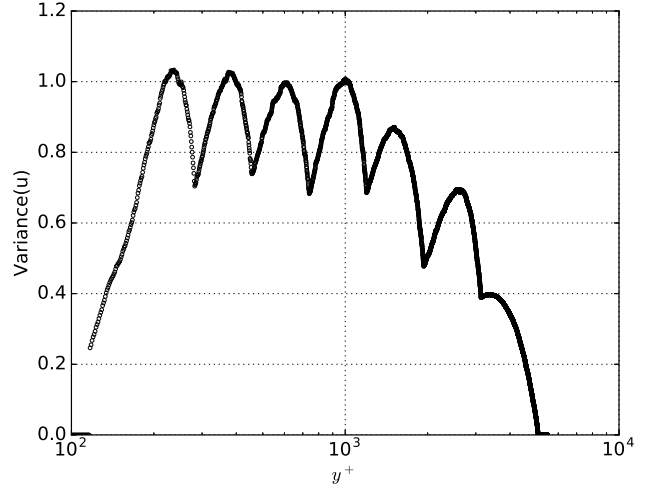


FIG. 12. Variance of streamwise velocity fluctuations for 5000 independent realizations with an uniform perturbation of $\pm 130\%$.

moments, however their amplitude are smaller compared

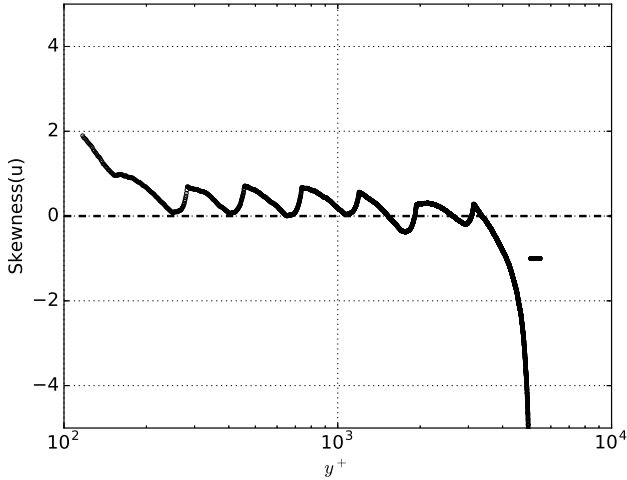


FIG. 13. Skewness of streamwise velocity fluctuations for 5000 independent realizations with an uniform perturbation of $\pm 130\%$ (open circles). The skewness for a Gaussian distribution is plotted in dotted lines as a reference.

with the gaussian distribution for $\sigma = 0.4$. Fig. 13 shows the skewness of the streamwise velocity for an uniform distribution. A strong agreement in the main features between the numerical simulation and the experimental skewness is observed, in brief the skewness follows a pseudo-Gaussian trend in the inertial region , then it increases up to reach its maximum negative value in the upper limit of the boundary layer $y^+ = \delta^+$ to after finally decay to zero in the free-stream region. Fourth order moment is illustrated in Fig. 14, the trend is in complete concordance with the experimental data if the small oscillations are neglected. Further exploration is needed to improve the right behaviour in the upper and lower limits of the inertial region.

-
- [1] C. D. Meinhart and R. J. Adrian, Physics of Fluids **7**, 694 (1995).
 - [2] C. M. de Silva, N. Hutchins, and I. Marusic, Journal of Fluid Mechanics **786**, 309 (2016).
 - [3] R. J. Adrian, C. D. Meinhart, and C. D. Tomkins, Journal of Fluid Mechanics **422**, 1 (2000).
 - [4] P. Priyadarshana, J. Klewicki, S. Treat, and J. Foss, Journal of Fluid Mechanics **570**, 307 (2007).
 - [5] J. Klewicki, P. Fife, T. Wei, and P. McMurtry, Philosophical Transactions of the Royal Society of London A: Mathematical, Physical and Engineering Sciences **365**, 823 (2007).
 - [6] P. Vincenti, J. Klewicki, C. Morrill-Winter, C. M. White, and M. Wosnik, Experiments in Fluids **54**, 1 (2013).
 - [7] J. F. Morrison, B. J. McKeon, W. Jiang, and A. J. Smits, Journal of Fluid Mechanics **508**, 99 (2004).
 - [8] T. Sauer, *Numerical Analysis*, 2nd ed. (Pearson, Boston, MA, 2011).

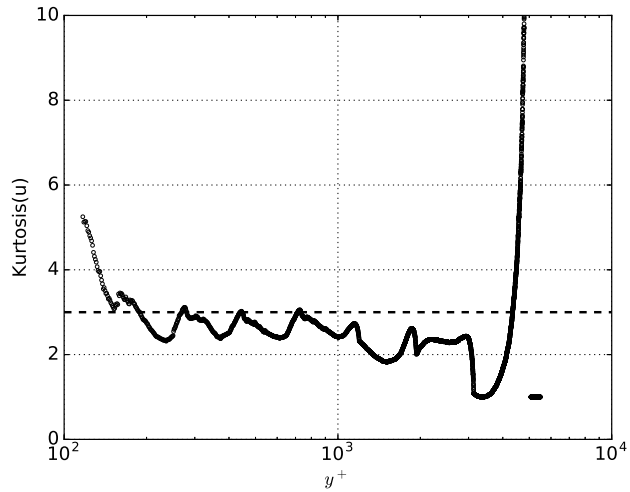


FIG. 14. Kurtosis of streamwise velocity fluctuations for 5000 independent realizations with a uniform perturbation of $\pm 130\%$ (open circles). The kurtosis for a Gaussian distribution is plotted in dotted lines as a reference.